From condensed-matter theory to subwavelength physics

Habib Ammari

Department of Mathematics, ETH Zürich

Subwavelength physics

- Subwavelength signal manipulation: revolutionizing nanotechnology; applications in wireless communications, biomedical superresolution imaging and quantum computing.
- Transpose demonstrated quantum phenomena to classical waves at subwavelength scales.
- Condensed-matter physics
  - Topological defects; Phase transitions; Hall effect; Localized states: Thouless, Duncan, Haldane, Kosterlitz, Anderson.
  - Systems of particles;
  - Hamiltonians; Tight-binding and Nearest-neighborhood approximations.
- Subwavelength physics
  - Systems of subwavelength resonators; PDE models; Capacitance matrix approximations; strong and long-range interactions in subwavelength resonator systems.

Single subwavelength resonator

- PDE model for a single subwavelength resonator:

$$
\begin{cases}
\Delta u + \omega^2 \dfrac{\rho}{\kappa} u = 0 \quad \text{in} \quad \mathbb{R}^3 \setminus \overline{D}, \\
\Delta u + \omega^2 \dfrac{\rho_r}{\kappa_r} u = 0 \quad \text{in} \quad D, \\
u|_+ = u|_- \quad \text{on} \quad \partial D, \\
\dfrac{\rho_r}{\rho} \dfrac{\partial u}{\partial \nu}\bigg|_+ = \dfrac{\partial u}{\partial \nu}\bigg|_- \quad \text{on} \quad \partial D, \\
u \text{ satisfies the (outgoing) Sommerfeld radiation condition.}
\end{cases}
$$

- κ_r, ρ_r, κ, ρ: material parameters inside and outside D.
- $k_r = \omega\sqrt{\rho_r/\kappa_r}$; $v_r = \sqrt{\kappa_r/\rho_r}$; $k = \omega\sqrt{\rho/\kappa}$; $v = \sqrt{\kappa/\rho}$.
- $v_r, v = O(1)$; High contrast: $\delta := |\rho_r/\rho| \ll 1$.
- Given δ, a subwavelength resonant frequency $\omega = \omega(\delta) \in \mathbb{C}$:
  - (i) there exists a non-trivial solution to the PDE model;
  - (ii) ω depends continuously on δ and satisfies $\omega \to 0$ as $\delta \to 0$.

Dilute systems of subwavelength resonators[1]

- Subwavelength resonance frequency for a single subwavelength resonator:

$$\underbrace{\sqrt{\frac{\mathrm{Cap}_D}{|D|}} v_r \sqrt{\delta}}_{:=\omega_M} + i \underbrace{\left(-\frac{\mathrm{Cap}_D^2 v_r^2}{8\pi v |D|}\delta\right)}_{:=\tau_M} + O(\delta^{\frac{3}{2}}).$$

- Capacity $\mathrm{Cap}_D := -\int_{\partial D} \mathcal{S}_D^{-1}[\chi_{\partial D}]\, d\sigma$; $\mathcal{S}_D[\phi] = \int_{\partial D} G(x-y)\phi(y)\, d\sigma(y)$.
- Effective operator for a dilute system: $\Delta + k^2 + V(x)$;
- $V(x) = \dfrac{1}{(\frac{\omega_M}{\omega})^2 - 1} \Lambda \widetilde{V}(x)$;
- Λ: depends only on the volume fraction of the subwavelength resonators;
- $\widetilde{V}$: depends only on the distribution of the centers of the subwavelength resonators.

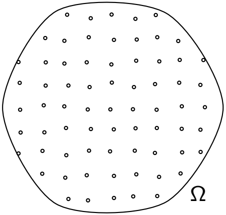

[1] with H. Zhang, SIAM J. Math. Anal., 2017.

Finite systems of strongly interacting resonators[2]

- $D = D_1 \cup \cdots \cup D_N$;
- v_i: wave speed in D_i;
- $\delta_i = O(\delta), \quad |\delta| \ll 1$, $i = 1, \ldots, N$;
- $\chi_{\partial D_j}$: characteristic function of ∂D_j.

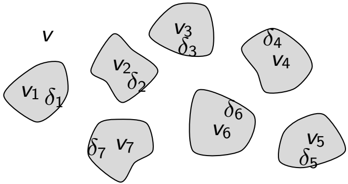

- Capacitance matrix: $C_{ij} = -\int_{\partial D_i} \underbrace{(\mathcal{S}_D)^{-1}[\chi_{\partial D_j}]}_{:=\psi_j} \, d\sigma, \quad i,j = 1, \ldots, N.$

- C: symmetric; positive definite; strictly diagonally dominant; $C_{ij} \sim 1/|i-j|$.
- Generalized capacitance matrix: $\mathcal{C} = VC$; $V = \mathrm{diag}(\delta_i v_i^2/|D_i|)$.
- Characterization of the subwavelength resonant frequencies:

$$\omega_n = \sqrt{\lambda_n} + O(\delta), \quad n = 1, \ldots, N;$$

- $\{\lambda_n : n = 1, \ldots, N\}$: eigenvalues of $\mathcal{C}$, which satisfy $\lambda_n = O(\delta)$ as $\delta \to 0$.

[2]with B. Davies, E. Hiltunen, Submitted, 2021.

Finite systems of strongly interacting resonators

- Comparison between the values computed using Muller's method and the multipole expansion method to discretize the full boundary integral equation $\mathcal{A}(\omega, \delta)[\Psi] = 0$ and the values computed using the discrete approximation.
- Subwavelength resonant frequencies of a system of $N = 10$ spherical resonators; Each resonator has unit radius and $\delta = 1/5000$.
- Computations using the full multipole method took 41 seconds while the discrete approximation took just 0.02 seconds, on the same computer.

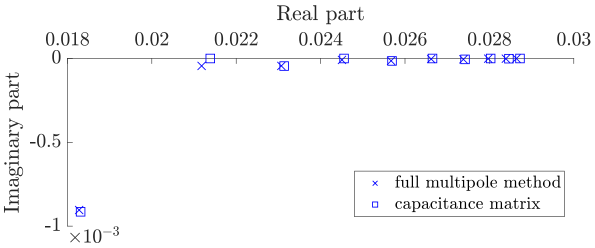

Finite systems of strongly interacting resonators

- Characterization of the subwavelength resonant modes:
  - $\mathbf{v}_n$: eigenvector of $\mathcal{C}$ associated to λ_n.
  - Resonant mode u_n associated to ω_n:

$$u_n(x) = \begin{cases} \mathbf{v}_n \cdot \mathbf{S}_D^k(x) + O(\delta^{1/2}), & x \in \mathbb{R}^3 \setminus \overline{D}, \\ \mathbf{v}_n \cdot \mathbf{S}_D^{k_i}(x) + O(\delta^{1/2}), & x \in D_i. \end{cases}$$

  - $\mathbf{S}_D^k : \mathbb{R}^3 \to \mathbb{C}^N$:

$$\mathbf{S}_D^k(x) = \begin{pmatrix} \mathcal{S}_D^k[\psi_1](x) \\ \vdots \\ \mathcal{S}_D^k[\psi_N](x) \end{pmatrix}, \quad x \in \mathbb{R}^3 \setminus \partial D;$$

  - $\psi_i := (\mathcal{S}_D)^{-1}[\chi_{\partial D_i}]$.
  - $\mathcal{S}_D^k$: single-layer potential associated with G_k: outgoing fundamental solution of the Helmholtz operator $\Delta + k^2$.

Exceptional points for PT-symmetric dimers[3]

- Parity-time-symmetric system: $D_1 = -D_2$ and $v_1^2\delta_1 = \overline{v_2^2\delta_2}$

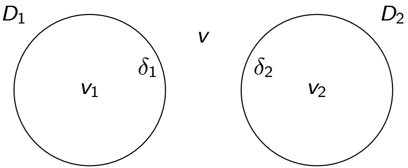

- $v_1^2\delta_1 := a+ib$, $v_2^2\delta_2 := a-ib$, for $a, b \in \mathbb{R}$; $|b|$: magnitude of the gain and the loss.
- Asymptotic exceptional points: There is a magnitude of the gain/loss such that resonant frequencies and corresponding eigenmodes coincide to leading order in δ.
- $\mathcal{PT}$-symmetry forces the spectrum of the capacitance matrix to be conjugate symmetric.
- The operator in the PDE model: not $\mathcal{PT}$-symmetric due to the radiation condition $\Rightarrow$ approximate nature of the exceptional points.

[3]with B. Davies, E.O. Hiltunen, H. Lee, S. Yu, Studies in Appl. Math., 2021.

Exceptional points for PT-symmetric dimers

- As $\delta \to 0$, $\omega_i = \sqrt{\lambda_i} + O(\delta), \quad i = 1, 2.$
- $$\lambda_i = \frac{1}{|D_1|}\left(aC_{11} + (-1)^i \sqrt{a^2 C_{12}^2 - b^2 (C_{11}^2 - C_{12}^2)}\right), \quad i = 1, 2.$$
- $b_0 = \frac{aC_{12}}{\sqrt{C_{11}^2 - C_{12}^2}}$ corresponds to the point where $\mathcal{C}$ has a double eigenvalue corresponding to a one-dimensional eigenspace.

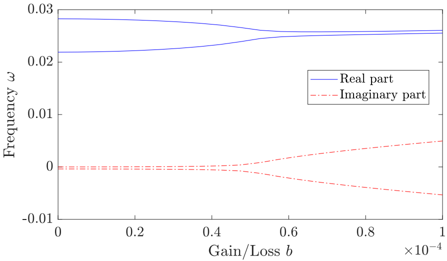

Periodic systems of resonators

- d_l: dimension of periodicity of the lattice. d: dimension of the ambient space. $P_\perp : \mathbb{R}^d \to \mathbb{R}^{d-d_l}$: projection onto the last $d - d_l$ coordinates.
- Three different cases:
  - $d - d_l = 0$: crystal;
  - $d - d_l = 1$: screen;
  - $d - d_l = 2$: chain.

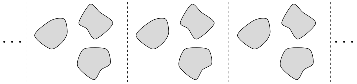

- Λ: periodic lattice; $l_1, \ldots, l_{d_l}$: lattice vectors ($P_\perp l_i = 0, i = 1, \ldots, d_l$).

$$\Lambda := \{ m_1 l_1 + \ldots + m_{d_l} l_{d_l} | m_i \in \mathbb{Z} \}.$$

- Y: fundamental domain

$$Y := \{ c_1 l_1 + \ldots + c_{d_l} l_{d_l} | 0 \le c_1, \ldots, c_{d_l} \le 1 \}.$$

- Λ^*: dual lattice of Λ generated by $\alpha_1, \ldots, \alpha_{d_l}$ satisfying $\alpha_i \cdot l_j = 2\pi\delta_{ij}$, $P_\perp \alpha_i = 0, i = 1, \ldots, d_l$;
- Brillouin zone $Y^* := (\mathbb{R}^{d_l} \times \{\mathbf{0}\}) / \Lambda^*$; $\mathbf{0}$: zero-vector in $\mathbb{R}^{d-d_l}$.

Subwavelength spectrum

- Periodically repeated i^{th} resonator $\mathcal{D}_i$ and the full periodic structure $\mathcal{D}$:

$$\mathcal{D}_i = \bigcup_{m \in \Lambda} D_i + m, \qquad \mathcal{D} = \bigcup_{i=1}^{N} \mathcal{D}_i.$$

- Subwavelength spectrum of the original problem:

$$\sigma = \bigcup_{\alpha \in Y^*} \sigma(\alpha).$$

- For $\alpha \in Y^*$, $\sigma(\alpha)$, the subwavelength spectrum of the quasiperiodic problem, consists of N discrete values ω_i^α:

$$\sigma(\alpha) = \{\omega_i^\alpha\}_{i=1}^N.$$

- $\alpha \mapsto \omega_i^\alpha$: band functions.

First radiation continuum

- Subwavelength band structure of a chain with two resonators in the unit cell.

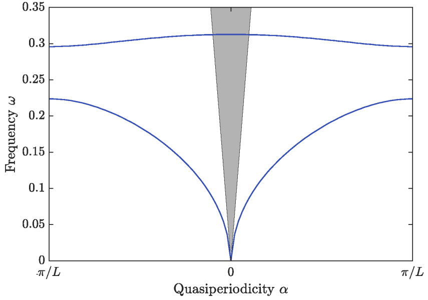

- Shaded region is the first radiation continuum, defined by

$$|\alpha| < \frac{\omega}{v} < \inf_{q \in \Lambda^* \setminus \{0\}} |\alpha + q|;$$

- Waves in this regime are propagating far away from the structure.
- Unshaded region corresponds to evanescent modes.

Subwavelength band functions

- Assume $|\alpha| > c > 0$ for some constant c independent of ω and δ. As $\delta \to 0$, the N subwavelength resonant frequencies satisfy the asymptotic formula

$$\omega_n^\alpha = \sqrt{\lambda_n^\alpha} + O(\delta^{3/2}), \quad n = 1, \ldots, N.$$

- $\{\lambda_n^\alpha : n = 1, \ldots, N\}$: eigenvalues of the generalized quasiperiodic capacitance matrix $\mathcal{C}^\alpha$, which satisfy $\lambda_n^\alpha = O(\delta)$ as $\delta \to 0$.
- Resonant mode u_n^α associated to ω_n^α:

$$u_n^\alpha(x) = \begin{cases} \mathbf{v}_n^\alpha \cdot \mathbf{S}_D^{\alpha,k}(x) + O(\delta^{1/2}), & x \in \mathbb{R}^d \setminus \overline{\mathcal{D}}, \\ \mathbf{v}_n^\alpha \cdot \mathbf{S}_D^{\alpha,k_i}(x) + O(\delta^{1/2}), & x \in \mathcal{D}_i. \end{cases}$$

- $\mathbf{S}_D^{\alpha,k} : \mathbb{R}^d \to \mathbb{C}^N$:

$$\mathbf{S}_D^{\alpha,k}(x) = \begin{pmatrix} \mathcal{S}_D^{\alpha,k}[\psi_1^\alpha](x) \\ \vdots \\ \mathcal{S}_D^{\alpha,k}[\psi_N^\alpha](x) \end{pmatrix}, \quad x \in \mathbb{R}^d \setminus \partial\mathcal{D},$$

with $\psi_i^\alpha := (\mathcal{S}_D^{\alpha,0})^{-1}[\chi_{\partial D_i}]$.

Quasiperiodic capacitance matrix

- System of N resonators $D_1, \ldots, D_N$ in Y.
- Quasiperiodic capacitance matrix
  - For $\alpha \neq 0$, $C^\alpha = (C_{ij}^\alpha) \in \mathbb{C}^{N\times N}$:

$$C_{ij}^\alpha = -\int_{\partial D_i} (\mathcal{S}_D^{\alpha,0})^{-1}[\chi_{\partial D_j}]\, d\sigma, \quad i,j = 1,\ldots,N.$$

  - C^α: Hermitian.
- Generalized quasiperiodic capacitance matrix
  - For $\alpha \neq 0$, $\mathcal{C}^\alpha = (\mathcal{C}_{ij}^\alpha) \in \mathbb{C}^{N\times N}$:

$$\mathcal{C}_{ij}^\alpha = \frac{\delta_i v_i^2}{|D_i|} C_{ij}^\alpha, \quad i,j = 1,\ldots,N.$$

Quasiperiodic capacitance matrix

- Single layer potential associated with $G^{\alpha,k}$:

$$\mathcal{S}_D^{\alpha,k}[\phi] = \int_{\partial D} G^{\alpha,k}(x,y)\phi(y)\, d\sigma(y).$$

- Quasi-periodic Green's function:

$$G^{\alpha,k}(x,y) = \sum_{m\in\Lambda} \frac{e^{ik|x-y-m|}}{4\pi|x-y-m|} e^{i\alpha\cdot m}.$$

- Uniform convergence for x and y in compact sets of $\mathbb{R}^d$, $x \neq y$, and $k \neq |\alpha + q|$ for all $q \in \Lambda^*$.
- $\mathcal{S}_D^{\alpha,k} : L^2(\partial D) \to H^1(\partial D)$ is invertible if k is small enough and $k \neq |\alpha + q|$ for all $q \in \Lambda^*$.
- For $\alpha \neq 0$,

$$\mathcal{S}_D^{\alpha,k} = \mathcal{S}_D^{\alpha,0} + O(k^2) \quad \text{as } k \to 0.$$

Resonances in the first radiation continuum

- Resonances in the first radiation continuum $|\alpha| < k = \omega/v < \inf_{q\in\Lambda^*\setminus\{0\}}|\alpha+q|$.
- For any $\alpha_0 \in Y^*$ with $|\alpha_0| < 1/v$, $\left(\mathcal{S}_D^{\omega\alpha_0,\omega}\right)^{-1}$: holomorphic operator-valued function of ω in a neighbourhood of $\omega = 0$:

$$\left(\mathcal{S}_D^{\omega\alpha_0,\omega}\right)^{-1} = \mathcal{S}_0^{\alpha_0} + \omega\mathcal{S}_{-1}^{\alpha_0} + O(\omega^2) \text{ as } \omega \to 0.$$

- Periodic capacitance matrix: For α_0 with $|\alpha_0| < 1/v$:

$$C^0 = (C_{ij}^0) \in \mathbb{R}^{N\times N}, \quad C_{ij}^0 = -\int_{\partial D_j} \mathcal{S}_0^{\alpha_0}[\chi_{\partial D_i}] d\sigma.$$

- C^0: independent of α_0.
- Generalized periodic capacitance matrix:

$$\mathcal{C}_{ij}^0 = \frac{\delta_i v_i^2}{|D_i|} C_{ij}^0, \quad i,j = 1,\ldots,N.$$

- Assume that $\alpha = \omega\alpha_0$ for some α_0 independent of ω and δ such that $|\alpha_0| < 1/v$. As $\delta \to 0$, there are N subwavelength resonant frequencies

$$\omega_n^\alpha = \sqrt{\lambda_n^0} + O(\delta), \quad n = 1,\ldots,N, \quad \{\lambda_n^0\}: \text{ eigenvalues of } \mathcal{C}^0.$$

Subwavelength bandgap opening[5]

- Square crystal:

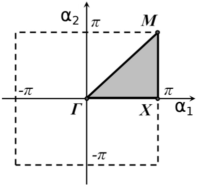

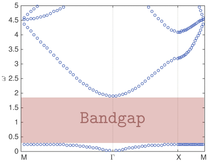

- Two-scale behaviour of the resonant mode for α close to (π, π): rapidly oscillating on the crystal scale, and a large scale envelope which satisfies a homogenized equation[4].

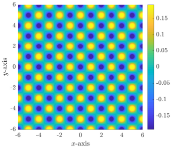

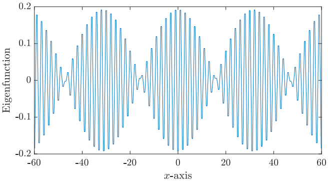

[4]with H. Lee, H. Zhang, SIAM J. Math. Anal., 2018.
[5]with B. Fitzpatrick, H. Lee, S. Yu, H. Zhang, J. Diff. Equat., 2017.

Honeycomb lattice of subwavelength resonators[6]

- Honeycomb lattice:

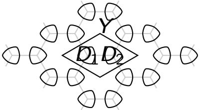

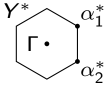

- At $\alpha = \alpha^*$, the first eigenfrequency $\omega^* := \omega(\alpha^*)$ of multiplicity 2.
- Conical behavior of subwavelength bands: The first band and the second band form a Dirac cone at α^*, i.e.,

$$\omega_1(\alpha) = \omega(\alpha^*) - \lambda|\alpha - \alpha^*|[1 + O(|\alpha - \alpha^*|)],$$
$$\omega_2(\alpha) = \omega(\alpha^*) + \lambda|\alpha - \alpha^*|[1 + O(|\alpha - \alpha^*|)];$$

$\lambda = |c|\sqrt{\delta}\lambda_0 \neq 0$ for sufficiently small δ.

- Dirac point at $\alpha = \alpha^*$.

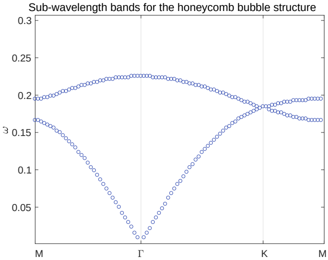

[6] with B. Fitzpatrick, E.O. Hiltunen, H. Lee, S. Yu, SIAM J. Math. Anal., 2020.

Honeycomb lattice of subwavelength resonators[7]

- For α close to α^*, eigenmodes:

$$\tilde{u}_1(x)S_1(\tfrac{x}{s}) + \tilde{u}_2(x)S_2(\tfrac{x}{s}) + O(\delta + s);$$

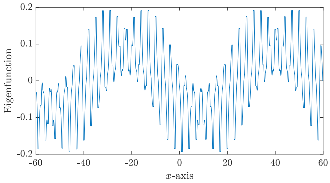

- Effective equation: $\tilde{u}_j$ satisfies

$$|c|^2\lambda_0^2\Delta\tilde{u}_j + \underbrace{\frac{(\omega-\omega^*)^2}{\delta}}_{\text{near zero}}\tilde{u}_j = 0.$$

- Dirac equation:

$$\lambda_0 \begin{bmatrix} 0 & (-ci)(\partial_1 - i\partial_2) \\ (-\bar{c}i)(\partial_1 + i\partial_2) & 0 \end{bmatrix} \begin{bmatrix} \tilde{u}_1 \\ \tilde{u}_2 \end{bmatrix} = \frac{\omega-\omega^*}{\sqrt{\delta}} \begin{bmatrix} \tilde{u}_1 \\ \tilde{u}_2 \end{bmatrix}.$$

- Zero-phase shift propagation.
- High transmittance $\Leftarrow$ Dirac cone near Γ.

[7] with E.O. Hiltunen, S. Yu, Arch. Ration. Mech. Anal., 2020.

Subwavelength trapping and guiding of waves

- Introduce a defect to a periodic arrangement of subwavelength resonators.

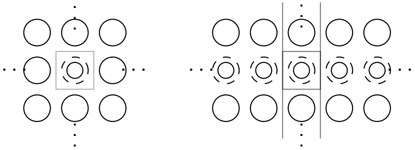

- Create a defect mode[8] or a defect band[9] inside the subwavelength band gap of the unperturbed structure.

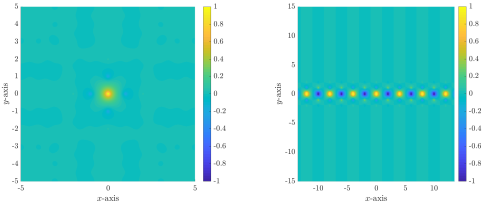

[8]with E.O. Hiltunen, S. Yu, SIAM J. Appl. Math., 2018.
[9]with E.O. Hiltunen, S. Yu, J. Eur. Math. Soc., 2022.

Topological defects

- Sensitivity to imperfections in the crystal's design:

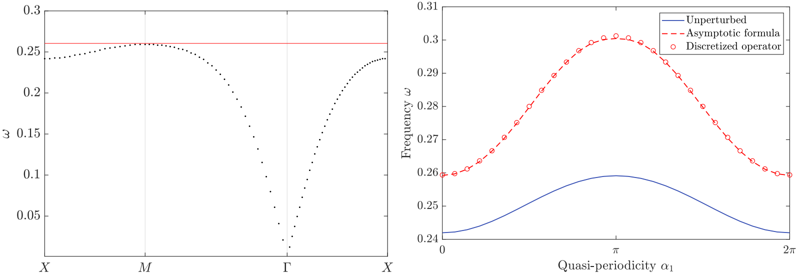

- Goal: design subwavelength wave guides whose properties are robust with respect to imperfections.
- Idea: Topological invariant which captures the crystal's wave propagation properties.

Topological defects

- Bulk-boundary correspondence:
  - Take two crystals with topologically different wave propagation properties (different values of the topological invariant);
  - Join half of crystal A to half of crystal B;
  - At the interface, a topologically protected edge mode will exist[10].

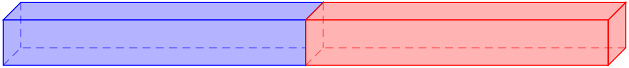

[10] with B. Davies, E.O. Hiltunen, S. Yu, J. Math. Pures Appl., 2020.

Topological defects

- An infinite chain of resonator dimers:[11]

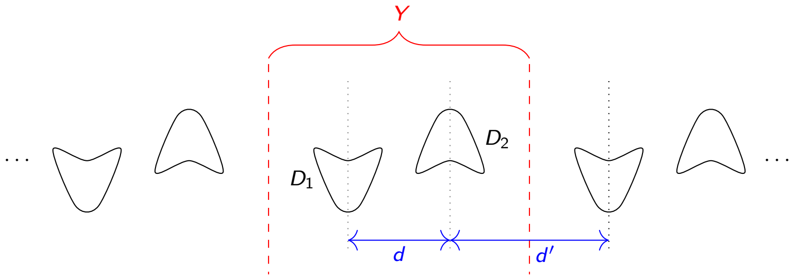

Two assumptions of geometric symmetry:

- dimer is symmetric, in the sense that $D(:= D_1 \cup D_2) = -D$,
- each resonator has reflective symmetry.

[11] Analogue of the Su-Schrieffer-Heeger model in topological insulator theory in quantum mechanics.

Topological defects

- The Zak phase:

$$\varphi_n^z := \int_{Y^*} A_n(\alpha)\, d\alpha; \quad Y^* = \mathbb{R}/2\pi\mathbb{Z} \simeq (-\pi, \pi] \quad \text{(first Brillouin zone)};$$

- Berry-Simon connection:

$$A_n(\alpha) := i \int_D u_n^\alpha \frac{\partial}{\partial \alpha} \overline{u}_n^\alpha \, dx; \quad n = 1, 2.$$

- For any $\alpha_1, \alpha_2 \in Y^*$, parallel transport from α_1 to α_2 gives $u_n^{\alpha_1} \mapsto e^{i\theta} u_n^{\alpha_2}$, where θ is given by

$$\theta = \int_{\alpha_1}^{\alpha_2} A_n d\alpha.$$

- $\Rightarrow$ The Zak phase corresponds to parallel transport around the whole of Y^*.

Topological defects

- Quasi-periodic capacitance matrix: $C = (C_{ij}^{\alpha})_{i,j=1,2}$.
- The Zak phase is given by the change in the argument of C_{12}^{α} as α varies over the Brillouin zone:
$$\varphi_n^z = -\frac{1}{2}\left[\arg(C_{12}^{\alpha})\right]_{Y^*}.$$
- Further, it holds that
$$C_{12}^{\alpha\,\prime} = e^{-i\alpha} C_{12}^{\alpha}, \Rightarrow \text{if } d = d' \text{then } C_{12}^{\pi} = 0,$$
where the prime denotes that d and d' have been swapped.
- Thus,
$$|\varphi_n^{z\,\prime} - \varphi_n^z| = \pi,$$
i.e. the cases $d > d'$ and $d < d'$ have different Zak phases.

Topological defects

- Dilute computations: Assume that the dimer is a rescaling of fixed domains B_1 and B_2:

$$D_1 = \epsilon B_1 - \left(\frac{d}{2}, 0, 0\right), \quad D_2 = \epsilon B_2 + \left(\frac{d}{2}, 0, 0\right),$$

  for $0 < \epsilon$.

- In the dilute regime, as $\epsilon \to 0$:

$$\varphi_n^z = \begin{cases} 0, & \text{if } \ d < d', \\ \pi, & \text{if } \ d > d', \end{cases}$$

- There exists a band gap for all $d \neq d'$,
- The dilute crystal has a degeneracy precisely when $d = d'$.
- The dispersion relation has a Dirac cone at $\alpha = \pi$.
- Band inversion occurs between $d < d'$ and $d > d'$.

Topological defects

- Band inversion:

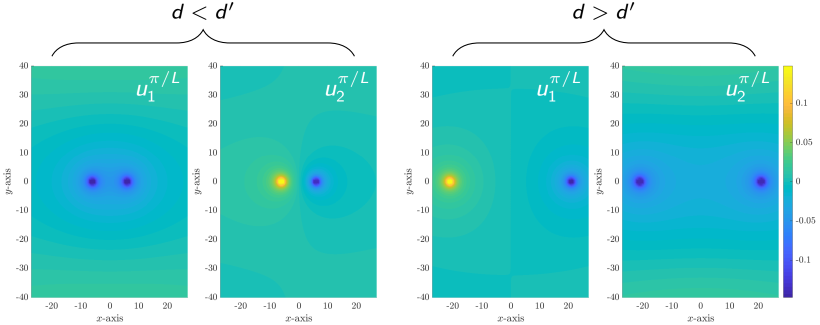

The monopole/dipole natures of the 1st and 2nd eigenmodes have swapped between the $d < d'$ and $d > d'$ regimes.

Topological defects

- A finite chain of resonators

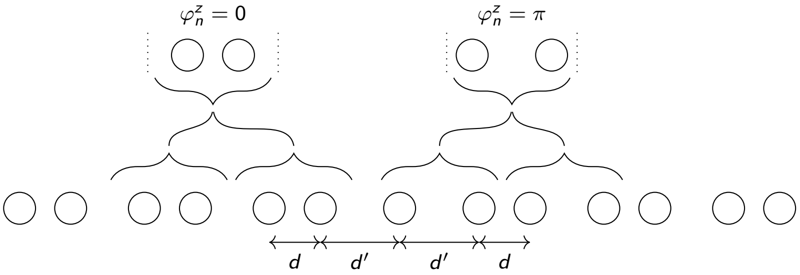

- Capacitance matrix of the finite chain $D = \bigcup_{l=1}^N D_l$:

$$C = (C_{ij}), \quad C_{ij} := -\int_{\partial D_j} (\mathcal{S}_D)^{-1}[\chi_{\partial D_i}], \quad i,j = 1,\ldots,N.$$

- Odd number of resonators $\Rightarrow$ odd number of eigenvalues; middle frequency: midgap frequency $\Rightarrow$ robust to imperfections.

Topological defects

- Finite chain - localization: There is a localized eigenmode

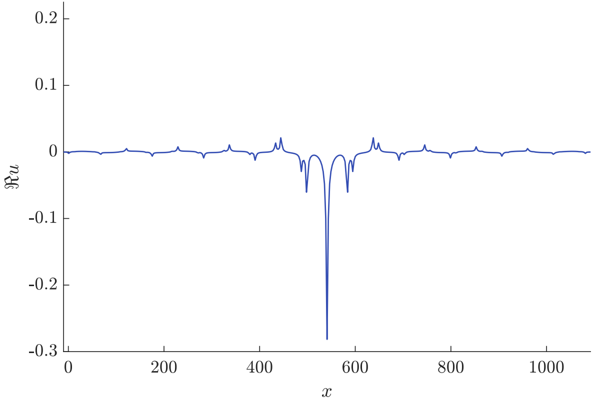

Topological defects

- Finite chain–stability to imperfections: Simulation of band gap frequency (red) and bulk frequencies (black) with Gaussian $\mathcal{N}(0, \sigma^2)$ errors added to the resonator positions. σ: expressed as a percentage of the average resonator separation.
- Even for relatively small errors, the frequency associated with the point defect mode exhibits poor stability and is easily lost amongst the bulk frequencies.

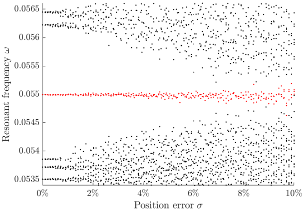

Finite chain with topological interface

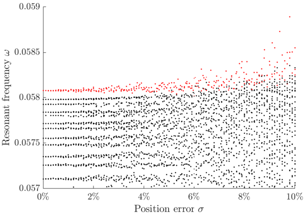

Classical, point defect chain.

Edge modes in a dislocated chain[12]

- A second approach for creating robust localized subwavelength modes:
  - We start with an array of pairs of subwavelength resonators, known to have a subwavelength band gap. A dislocation (with size $d > 0$) is introduced to create mid-gap frequencies.

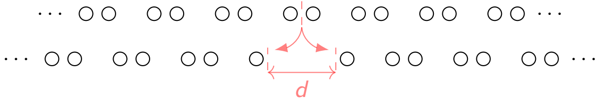

[12] with B. Davies, E.O. Hiltunen, J. London Math. Soc., 2022.

Edge modes in a dislocated chain

- As the dislocation size d increases from zero, a mid-gap frequency appears from each edge of the subwavelength band gap. These two frequencies converge to a single value within the subwavelength band gap as $d \to \infty$.

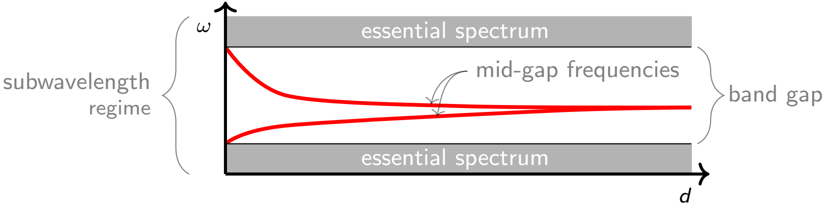

Non-Hermitian band inversion and edge modes[13]

- Edge modes in the non-Hermitian case:
  - Protected edge modes in crystals where the periodic geometry is intact, and a defect is placed in the parameters.
  - A topological winding number: the non-Hermitian Zak phase, which describes the winding of the complex eigenvalues.
  - Exceptional point degeneracies can open into non-trivial band gaps enabling topologically protected non-Hermitian edge modes.

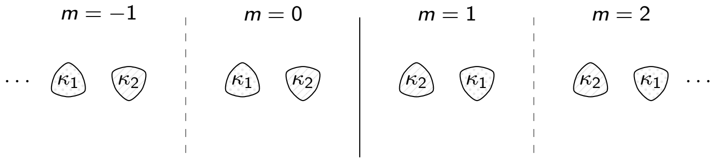

[13] with E.O. Hiltunen, submitted, 2021.

Non-Hermitian band inversion and edge modes

- Generalized quasiperiodic capacitance matrix:

$$\mathcal{C}^\alpha = \frac{1}{\rho|D_1|}\begin{pmatrix} \kappa_1 C_{11}^\alpha & \kappa_1 C_{12}^\alpha \\ \kappa_2 C_{21}^\alpha & \kappa_2 C_{22}^\alpha \end{pmatrix}.$$

- Eigenvalues λ_i^α of $\mathcal{C}^\alpha$:

$$\lambda_j^\alpha = \frac{1}{\rho|D_1|}\left(C_{11}^\alpha \frac{\kappa_1+\kappa_2}{2} + (-1)^j \sqrt{\left(\frac{\kappa_1-\kappa_2}{2}\right)^2 (C_{11}^\alpha)^2 + \kappa_1\kappa_2 |C_{12}^\alpha|^2}\right).$$

- As $\delta \to 0$, $\omega_i^\alpha = \sqrt{\lambda_i^\alpha} + O(\delta), \quad i = 1, 2.$
- Exceptional point degeneracy to occur for small δ: $\lambda_1^\alpha = \lambda_2^\alpha$ at some $\alpha \in Y^*$.

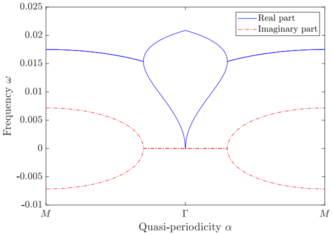

Non-Hermitian band inversion and edge modes

- Non-Hermitian Zak phase: u_j^α: right eigenmode; v_j^α: left eigenmode corresponding to $\overline{\omega_j^\alpha}$,

$$\varphi_j^{\mathrm{zak}} := \frac{i}{2}\int_{Y^*}\left(\left\langle v_j^\alpha, \frac{\partial u_j^\alpha}{\partial\alpha}\right\rangle + \left\langle u_j^\alpha, \frac{\partial v_j^\alpha}{\partial\alpha}\right\rangle\right) d\alpha.$$

- Hermitian counterpart of the structure is topologically trivial:

$$\varphi_j^{\mathrm{zak}}(\mathrm{Re}(\kappa_1), \mathrm{Re}(\kappa_2)) = 0.$$

- $\varphi_j^{\mathrm{zak}}(\kappa_1, \kappa_2) = -\varphi_j^{\mathrm{zak}}(\kappa_2, \kappa_1) + O(\delta), \quad \varphi_j^{\mathrm{zak}}(\overline{\kappa_1}, \overline{\kappa_2}) = \varphi_j^{\mathrm{zak}}(\kappa_1, \kappa_2) + O(\delta).$
- $\Rightarrow$ If $\kappa_1 = \overline{\kappa_2} := \kappa$, $\varphi_j^{\mathrm{zak}}(\kappa, \overline{\kappa}) = O(\delta)$.
- Exceptional point degeneracy occurs when $\kappa_1 = \overline{\kappa_2} = \kappa$ for sufficiently large κ:
  - $\beta_1 = C_{11}^\pi + C_{12}^\pi$, $\beta_2 = 2C_{11}^0$; $l = (\beta_1 + \beta_2)/(\beta_2 - \beta_1)$.
  - If $\kappa_1 = \overline{\kappa_2} := \kappa$ with $|\mathrm{Im}(\kappa)| \leq \frac{\mathrm{Re}(\kappa)}{\sqrt{l^2-1}}$ (unbroken $\mathcal{PT}$-symmetry), the structure does not support localized modes in the subwavelength regime.
  - If $\kappa_1 = \overline{\kappa_2} := \kappa$ with $|\mathrm{Im}(\kappa)| > \frac{\mathrm{Re}(\kappa)}{\sqrt{l^2-1}}$ (broken $\mathcal{PT}$-symmetry) or if $\kappa_1 \neq \overline{\kappa_2}$ (no $\mathcal{PT}$-symmetry): characterization of the localized mode in the subwavelength regime.

Non-Hermitian band inversion and edge modes

- Non-Hermitian Zak phase: not quantized but can nevertheless predict the existence of localized edge modes. Edge modes can be achieved by swapping κ_1 and κ_2 while keeping the distance between the resonators fixed.
- Purely non-Hermitian effect: as $\mathrm{Im}\kappa_1$ and $\mathrm{Im}\kappa_2 \to 0$, the effect disappears.

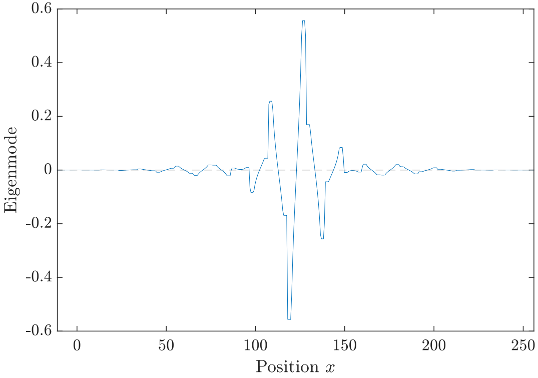

Topological phase transitions

Hermitian:

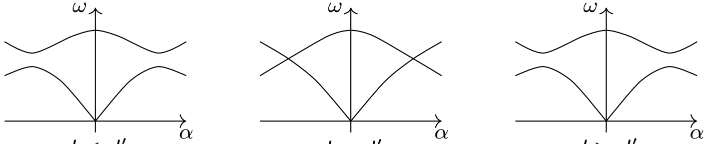

$d < d'$ No band inversion | $d = d'$ Dirac cone | $d > d'$ Full band inversion

Non-Hermitian:

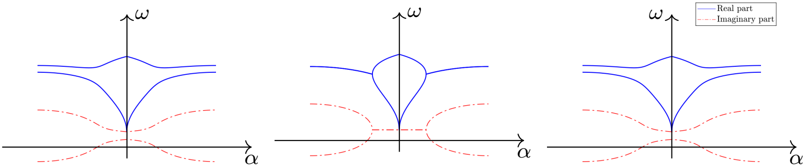

$|\kappa_1| < |\kappa_2|$ Partial inversion | $\kappa_1 = \overline{\kappa_2}$ Exceptional point | $|\kappa_1| > |\kappa_2|$ Partial inversion

Anderson localization[14]

- Strong localization in random media with long-range interactions.
- Scattering of waves by subwavelength resonators with randomly chosen material parameters reproduces the characteristic features of Anderson localization.
- Hybridization of subwavelength resonant modes is responsible for both the repulsion of energy levels as well as the phase transition, at which point eigenmode symmetries swap and very strong localization is possible.
- Characterization of the localized modes in terms of Laurent operators and generalized capacitance matrices.

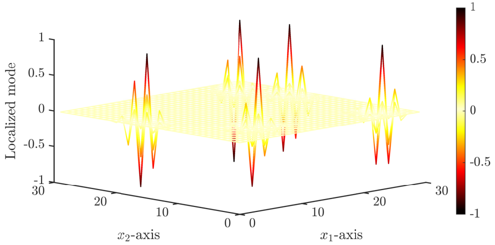

[14] with B. Davies, E.O. Hiltunen, submitted, 2022.

Anderson localization

- Characterization of localization: Any localized solution u corresponding to a subwavelength frequency $\omega = \omega_0 + O(\delta)$, satisfies

$$\mathcal{B}_m \sum_{n \in \Lambda} \mathcal{C}^{m-n} \mathbf{u}^n = \omega_0^2 \mathbf{u}^m,$$

for every $m \in \Lambda$ (real-space variable);

- $\mathcal{C}^m$: inverse Floquet transform of $\mathcal{C}^\alpha$ (real-space capacitance matrix); $\mathbf{u}^m \in \mathbb{R}^N$;
- $\mathcal{B}_m$: $N \times N$ diagonal matrix whose i^{th} entry is given by $b_i^m = 1 + x_i^m$; x_i^m: random perturbation of the material parameter of the resonator i in the cell m.

Laurent-operator formulation

- If $\Lambda = \mathbb{Z}$,

$$\mathfrak{B}\mathfrak{C}\mathfrak{u} = \omega_0^2 \mathfrak{u}.$$

- Doubly infinite matrices and vectors:

$$\mathfrak{C} = \begin{pmatrix} \ddots & \vdots & \vdots & \vdots & \vdots & \\ \cdots & \mathcal{C}^0 & \mathcal{C}^1 & \mathcal{C}^2 & \mathcal{C}^3 & \cdots \\ \cdots & \mathcal{C}^{-1} & \mathcal{C}^0 & \mathcal{C}^1 & \mathcal{C}^2 & \cdots \\ \cdots & \mathcal{C}^{-2} & \mathcal{C}^{-1} & \mathcal{C}^0 & \mathcal{C}^1 & \cdots \\ \cdots & \mathcal{C}^{-3} & \mathcal{C}^{-2} & \mathcal{C}^{-1} & \mathcal{C}^0 & \cdots \\ & \vdots & \vdots & \vdots & \vdots & \ddots \end{pmatrix}, \quad \mathfrak{u} = \begin{pmatrix} \vdots \\ \mathbf{u}^{-1} \\ \mathbf{u}^0 \\ \mathbf{u}^1 \\ \mathbf{u}^2 \\ \vdots \end{pmatrix}, \quad \mathfrak{B} = \begin{pmatrix} \ddots & \vdots & \vdots & \vdots & \vdots & \\ \cdots & \mathcal{B}_{-1} & 0 & 0 & 0 & \cdots \\ \cdots & 0 & \mathcal{B}_0 & 0 & 0 & \cdots \\ \cdots & 0 & 0 & \mathcal{B}_1 & 0 & \cdots \\ \cdots & 0 & 0 & 0 & \mathcal{B}_2 & \cdots \\ & \vdots & \vdots & \vdots & \vdots & \ddots \end{pmatrix}.$$

- $\mathfrak{C}$: (block) Laurent operator corresponding to the symbol $\mathcal{C}^\alpha$.
- A localized mode corresponds to an eigenvalue of the operator $\mathfrak{B}\mathfrak{C}$.
- In the periodic case (when $\mathfrak{B} = I$), the spectrum of the Laurent operator $\mathfrak{C}$ is continuous and does not contain eigenvalues, so there are no localized modes.
- The operator $\mathfrak{B}\mathfrak{C}$ might have a pure-point spectrum in the non-periodic case.

Toeplitz matrix formulation for compact defects

- Compact defects: $\mathcal{B}_m$ are identity for all but finitely many m; $0 \leq m \leq M$.
- X_m: diagonal matrix with entries x_i^m.
- (Block) Toeplitz matrix formulation: ω_0 corresponds to a localized mode iff

$$\det\big(I - \mathcal{X}\mathcal{T}(\omega_0)\big) = 0.$$

- $\mathcal{X}$: block-diagonal matrix with entries X_m;
- $$\mathcal{T}(\omega) = \begin{pmatrix} T^0 & T^1 & T^2 & \cdots & T^M \\ T^{-1} & T^0 & T^1 & \cdots & T^{M-1} \\ T^{-2} & T^{-1} & T^0 & \cdots & T^{M-2} \\ \vdots & \vdots & \vdots & \ddots & \vdots \\ T^{-M} & T^{-(M-1)} & T^{-(M-2)} & \cdots & T^0 \end{pmatrix};$$
- $$T^m = -\frac{1}{|Y^*|}\int_{Y^*} e^{i\alpha m}\mathcal{C}^\alpha \left(\mathcal{C}^\alpha - \omega^2 I\right)^{-1} d\alpha.$$

Hybridization and level repulsion

- A single localized mode:

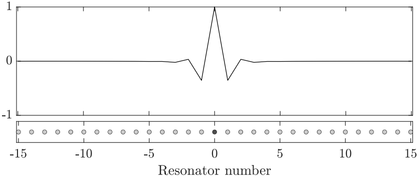

- Two localized modes (higher mode has a dipole (odd) symmetry while the lower mode has a monopole (even) symmetry):

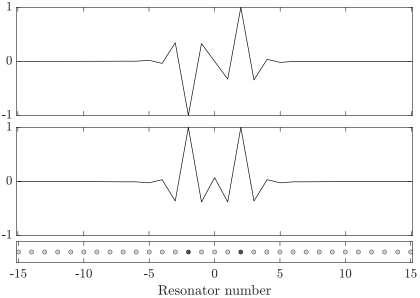

Hybridization and level repulsion

- The values of x_1 and x_2 are drawn independently from the uniform distribution $U[x - \sqrt{3}\sigma, x + \sqrt{3}\sigma]$.
- Level repulsion: introduction of random perturbations causes the average value of each mid-gap frequency to move further apart (and further apart the edge of the band gap):

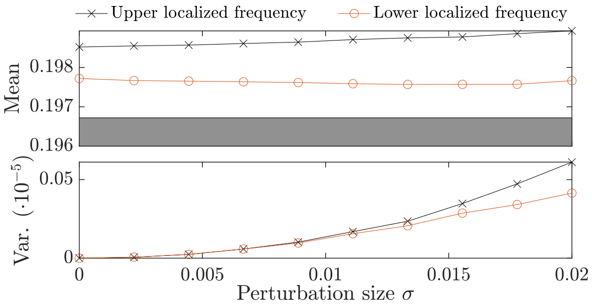

Phase transition and eigenmode symmetry swapping

- Doubly degenerate frequency: a transition point whereby the symmetries of the corresponding eigenmodes swap:

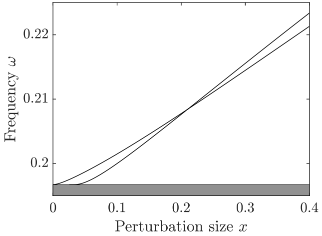

- Sharp peak at the transition point in the degree of localization:

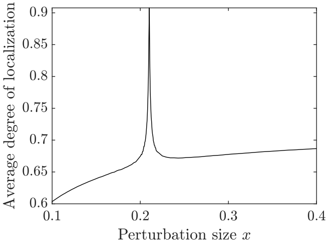

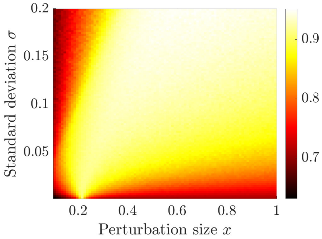

Time-modulated systems of resonators

- Wave equation in a time-modulated structure:

$$\left(\frac{\partial}{\partial t}\frac{1}{\kappa(x,t)}\frac{\partial}{\partial t} - \nabla\cdot\frac{1}{\rho(x,t)}\nabla\right)u(x,t) = 0, \quad x\in\mathbb{R}^d, t\in\mathbb{R}.$$

- Time-modulation of the resonators:

$$\kappa(x,t) = \begin{cases}\kappa, & x\in\mathbb{R}^d\setminus\overline{D},\\ \kappa_r\kappa_i(t), & x\in D_i,\end{cases}, \qquad \rho(x,t) = \begin{cases}\rho, & x\in\mathbb{R}^d\setminus\overline{D},\\ \rho_r\rho_i(t), & x\in D_i.\end{cases}$$

- $\rho_i(t)$ and $\kappa_i(t)$: modulation inside the i^{th} resonator D_i; ρ_i, κ_i: periodic with period T; $\kappa_i \in C^1(\mathbb{R})$ and $\kappa_i'(t) = O(\delta^{1/2})$ for each $i = 1, \ldots, N$.

Time-modulated systems of resonators

- Floquet transform in t:

$$\begin{cases} \left(\frac{\partial}{\partial t}\frac{1}{\kappa(x,t)}\frac{\partial}{\partial t} - \nabla\cdot\frac{1}{\rho(x,t)}\nabla\right)u(x,t) = 0, \\ u(x,t)e^{-i\omega t} \text{ is } T\text{-periodic in } t. \end{cases}$$

- Time-Brillouin zone: $\omega \in Y_t^* := \mathbb{C}/(\Omega\mathbb{Z})$; $\Omega = (2\pi)/T = O(\delta^{1/2})$.
- A quasifrequency is a subwavelength quasifrequency if the corresponding solution is essentially supported in the subwavelength frequency regime:

$$u(x,t) = e^{i\omega t}\sum_{n=-\infty}^{\infty} v_n(x)e^{in\Omega t}, \quad \omega : \text{Floquet exponent},$$

where

$$\omega \to 0 \text{ and } M\Omega \to 0 \text{ as } \delta \to 0,$$

for some integer-valued function $M = M(\delta)$ such that, as $\delta \to 0$, we have

$$\sum_{n=-\infty}^{\infty} \|v_n\|_{L^2(K)} = \sum_{n=-M}^{M} \|v_n\|_{L^2(K)} + o(1), \qquad K \text{ compact set containing } D.$$

Time-modulated systems of resonators[15]

- Capacitance matrix formulation of the problem:
  - As $\delta \to 0$, the quasifrequencies $\omega \in Y_t^*$ are, to leading order, given by the quasifrequencies of the system of ordinary differential equations:

$$\sum_{j=1}^{N} \mathcal{C}_{ij} c_j(t) = -\frac{1}{\rho_i(t)} \frac{d}{dt} \left(\frac{1}{\kappa_i(t)} \frac{d(\rho_i c_i)}{dt}(t) \right),$$

for $i = 1, \ldots, N$. ($c_j(t) = e^{i\omega t} \sum_n c_{j,n} e^{in\Omega t}$).

  - Rewrite as a system of Hill equations:

$$\Psi''(t) + M(t)\Psi(t) = 0.$$

  - Compute the Floquet exponents of the Hill system of equations.
  - If $\kappa_i(t) = 1, \rho_i(t) = \rho(t)$, $t \in \mathbb{R}, i = 1, \ldots, N$:

$$\Psi''(t) + \mathcal{C}\Psi(t) = 0.$$

  - $\Rightarrow$ Static case: Quasifrequencies $\omega_i = \sqrt{\lambda_i}$ at leading order in δ.

[15] with E.O. Hiltunen, J. Comp. Phys., 2021.

Space-time modulated systems of resonators

- Wave equation in a space-time modulated systems:

$$\left(\frac{\partial}{\partial t}\frac{1}{\kappa(x,t)}\frac{\partial}{\partial t} - \nabla\cdot\frac{1}{\rho(x,t)}\nabla\right)u(x,t) = 0, \quad x\in\mathbb{R}^d, t\in\mathbb{R}.$$

- Y: unit cell; $\mathcal{D} = \bigcup_{m\in\Lambda} D + m$; $\mathcal{D}_i = \bigcup_{m\in\Lambda} D_i + m$; $D_i, i = 1,\ldots,N$.
- Time-modulation of the resonators:

$$\kappa(x,t) = \begin{cases}\kappa, & x\in\mathbb{R}^d\setminus\overline{\mathcal{D}},\\ \kappa_r\kappa_i(t), & x\in\mathcal{D}_i,\end{cases}, \qquad \rho(x,t) = \begin{cases}\rho, & x\in\mathbb{R}^d\setminus\overline{\mathcal{D}},\\ \rho_r\rho_i(t), & x\in\mathcal{D}_i.\end{cases}$$

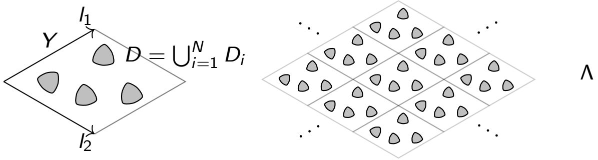

Space-time modulated systems of resonators

- Floquet transform in both x and t:

$$\begin{cases} \left(\frac{\partial}{\partial t} \frac{1}{\kappa(x,t)} \frac{\partial}{\partial t} - \nabla \cdot \frac{1}{\rho(x,t)} \nabla \right) u(x,t) = 0, \\ u(x,t)e^{-i\alpha\cdot x} \text{ is } \Lambda\text{-periodic in } x, \\ u(x,t)e^{-i\omega t} \text{ is } T\text{-periodic in } t. \end{cases}$$

- Space-Brillouin zone: $\alpha \in Y^* := \mathbb{R}^d / \Lambda^*$; Time-Brillouin zone: $\omega \in Y_t^* := \mathbb{C}/(\Omega\mathbb{Z})$; $\Omega = (2\pi)/T$.
- As $\delta \to 0$, the quasifrequencies $\omega = \omega(\alpha) \in Y_t^*$ are, to leading order, given by the quasifrequencies of the system of ordinary differential equations:

$$\sum_{j=1}^{N} \mathcal{C}_{ij}^{\alpha} c_j = -\frac{1}{\rho_i} \frac{d}{dt} \left(\frac{1}{\kappa_i} \frac{d(\rho_i c_i)}{dt} \right),$$

for $i = 1, \ldots, N$. $(c_j(t) = e^{i\omega t} \sum_n c_{j,n} e^{in\Omega t})$.

Pseudo-spin effect

- Trimer honeycomb lattice with phase-shifted time-modulations inside the trimers:

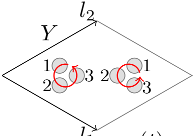

$$\kappa_j(t) = 1 + \epsilon \sin\left(\Omega t + \frac{2\pi j}{3}\right)$$

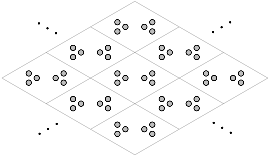

- Dirac cones at the origin of the Brillouin zone:

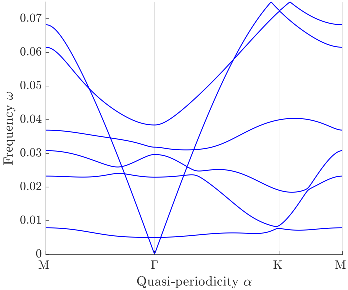

Unmodulated case

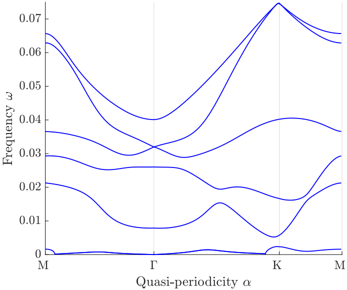

Modulated case

Non-reciprocal wave propagation and k-gaps

- Folding of the static band structure might create degenerate points:
- Degenerate points give rise to broken reciprocity[16] and k-gaps by time-modulation[17].
- Band functions of the static chain of trimers ($N = 3$), exhibiting degenerate points.

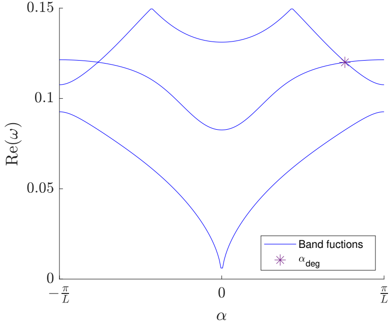

[16] with J. Cao, E.O. Hiltunen, SIAM MMS, 2022.
[17] with J. Cao, X. Zeng, Stud. Appl. Math., 2022.

Non-reciprocal wave propagation and k-gaps

- Non-reciprocal band gaps and k-gaps:

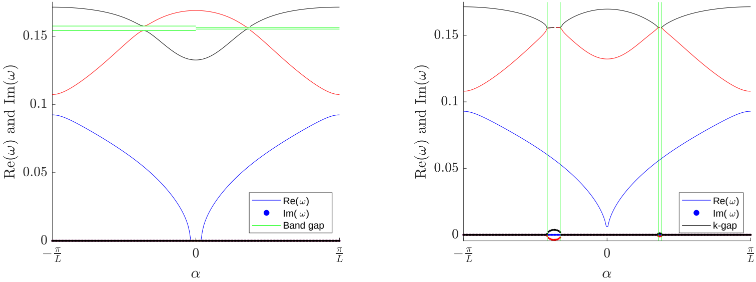

- Breaking reciprocity (time-reversal symmetry) $\Rightarrow$ non-symmetric bandgaps $\Rightarrow$ unidirectional excitation of the operating waves.
- Existence of k-gaps $\Rightarrow$ exponentially growing wave propagation.

Concluding remarks

- Quantitative explanation of the mechanisms behind the spectacular properties exhibited by subwavelength resonators in recent physical experiments:
  - **Hermitian systems**: Dirac degeneracies; Near-zero refraction; Topologically protected edge modes; Bound states in the continuum; Fano-resonances; Anderson localization.
  - **Non-Hermitian systems**: Exceptional point degeneracies; Non-quantized topological invariants; Unidirectional reflection and extraordinary transmission.
  - **Time-modulated systems**: Pseudo-spin effect; Double-zero refraction; Unidirectional guiding and broken time-reversal symmetry; One-way edge states; Amplified emission and k-gaps.
- Avenue for understanding the localization and topological properties of non-hermitian and time-modulated systems of subwavelength resonators.